

Chapter

Comparative Dosimetric Study between ^{60}Co and ^{192}Ir BEBIG High Dose Rate Sources, Used in Brachytherapy, Using Monte Carlo N-Particle Extended

Said Elboukhari, Khalid Yamni, Hmad Ouabi, Taoufiq Bouassa and Lahcen Ait Mlouk

Abstract

The purpose from this work is the investigation for dosimetric parameters of the two new BEBIG sources, ^{60}Co and ^{192}Ir used in high-dose-rate brachytherapy. According to the full report of AAPM and ESTRO; air-kerma strength, dose rate constant, radial dose function, and 2D along & away dose rates tables were calculated. Moreover, a comparison was made between the calculated dosimetric parameters for the HDR sources simulated in this study. We used the MCN-PX to investigate the dosimetric parameters of both sources. The geometry of each source was defined in the input program of MCNPX, and each simulation was performed with an appropriate number of particle histories to get an acceptable Type A statistical uncertainty. The results obtained were tabulated and presented in graphical format; these results show a good agreement with other previous studies. The comparison made between the two simulated sources in this work shows a minor difference observed in the generated 2D along & away tables for complementing the commissioning of these sources within a TPS. This difference is considered negligible by the clinical specialists.

Keywords: Co-60 versus Ir-192, Monte Carlo investigation, dosimetric comparison, HEBD working group

1. Introduction

The widespread sources in afterloading devices operated in high-dose-rate brachytherapy (HDR) are ^{60}Co and ^{192}Ir . This work aimed to investigate the dosimetric parameters for both HDR sources manufactured by BEBIG (Eckert & Ziegler BEBIG GmbH, Germany), ^{60}Co model: Co0.A86 and ^{192}Ir model: GI192M11, used in HDR

brachytherapy. According to the TG-43 U1 and HEBD Working Group Report, recommendations for high-energy photons emitting brachytherapy sources [1] were provided. The dosimetric parameters were calculated; The air-kerma strength, dose rate constant, radial dose function, and the 2D along & away dose rate table in Cartesian coordinates are calculated for both new BEBIG sources, except the 2D anisotropy function.

Several studies were made for the HDR brachytherapy sources with different geometries and nuclides; we have cited some of them in this work. Varieties of Monte Carlo codes have been used to investigate the HDR brachytherapy sources. The BEBIG Co0.A86 was investigated using Geant4 by Granero et al., (2007) [2], PENELOPE used by Guerrero et al., (2014) [3], a study was made by Anwarul et al., (2012) using the Monte Carlo code EGSnrc [4], and H. Badry et al., (2018) used EGS5 for simulation of the same source model [5].

For the ^{192}Ir model: GI192M11, a study was made by Perez-Calatayud et al., (2012) using the Geant3 Monte Carlo code [1], Geant4 was used by Granero et al., (2005) for the same source model [6]. The comparison was also made in the case of radial dose function with the results obtained for the source model BEBIG Ir2.A852 simulated by Granero et al., (2008) [7] and Belousov et al., (2014) [8]. The obtained results in this study were in good coherence with the published data. Monte Carlo simulations were provided following the records cited in the report of the research committee Task Group 268 from AAPM [9]. MCNPX code was already used in some previous studies we cited the use of the version: 2.4 by Alizadeh et al., (2015) for the HDR ^{192}Ir source Flexisource model [10]. Also, we have investigated the dosimetric parameters of the same ^{60}Co source in our previous study Elboukhari et al., (2020) using the version 2.7 of the code Monte Carlo N-Particles eXtended (MCNPX) [11], this new version of the code operates the new updated tables of cross sections from ENDF/B-VII.1 data. MCNPX is a general-purpose three-dimensional simulation tool providing the transports of 37 different particle types for criticality, dosimetry, shielding, detector response, and many other applications. On the contrary of previous MCNPX Monte Carlo codes, the version used in this work of MCNPX provided a high precision, and the uncertainties depending on cross section tables are considered negligible.

To evaluate the difference between the two sources simulated in this study within a clinical use, we have generated the 2D along & away tables for complementing the commissioning of these sources within a clinical treatment planning system. A minor difference was observed in the generated along & away dose rates for the range of distances considered in this work. These results could help in the choice of the appropriate nuclide to use in the treatment regarding operation costs and frequency for source change, especially for developing countries such as in North Africa. Also, different studies were performed concerning the clinic practice. A study of M. Andrassy et al., (2012) concerned the behavior in the treated volume [12]. In addition, the studies of Venselaar et al., (1996) and Candela et al., (2013) mentioned that the behavior of the two nuclides at shorter distances from the treated volume is different from that at larger distances [13, 14]. This result is also mentioned in the study of Strohmaier and Zwierzchowski in 2011 [15].

2. Materials and methods

In this study, Monte Carlo simulation for HDR brachytherapy sources was performed following the recommendations of the American Association of Physicists

in Medicine (AAPM) and the European Society for Radiotherapy and Oncology (ESTRO) in the HEBD working group report [1]. The formula proposed for 2D dose rates is:

$$\dot{D}(r, \theta) = S_k \Lambda \frac{G(r, \theta)}{G(r_0, \theta_0)} g_L(r) F(r, \theta) \quad (1)$$

Where:

- $\dot{D}(r, \theta)$ is the dose rate in water at the distance r in centimeters from a line source,;
- θ the polar angle specifying the point of interest;
- S_k the air-kerma strength in units of $\text{cGy cm}^2 \text{h}^{-1}$;
- Λ the dose rate constant expressed in $\text{cGy h}^{-1} \text{U}^{-1}$;
- $\frac{G(r, \theta)}{G(r_0, \theta_0)}$ is the geometry factor with the reference point ($r_0 = 1 \text{ cm}$ and $\theta_0 = 90^\circ$);
- $g_L(r)$ the radial dose function ($L = 3.5 \text{ mm}$ for both of the simulated sources in this work, Co0.A86 and GI192M11);
- $F(r, \theta)$ is the 2D anisotropy function.

3. Sources descriptions and geometries

3.1 ^{60}Co HDR source

The ^{60}Co HDR source (model Co0.A86, manufactured by BEBIG) was simulated in this work, and all the comparisons were made for the same source model. It is composed of homogeny cobalt 60 cylindrical core with $L = 3.5 \text{ mm}$ (length) and 0.5 mm in diameter (density = 8.09 gcm^{-3}). The active core is surrounded by air shell and encapsulated in a stainless steel cylindrical capsule with 0.15 mm thickness and 1 mm for the external diameter. We considered 0.9 mm and 2 mm for the source cable diameter and length, respectively, **Figure 1a**. The activity of the cobalt source used in this work was $A_0 = 81.56 \text{ GBq}$, and the cobalt 60 half-life is $t_{1/2} = 5.27 \text{ years}$. The density used for the stainless steel is 8.03 gcm^{-3} for both the capsule and the source cable [2].

3.2 ^{192}Ir HDR source

For the ^{192}Ir HDR source, model GI192M11, manufactured by E & Z BEBIG, was simulated in this work, the comparisons with the published data included: Ir2.A852, Flexisource, and GammaMed models. The BEBIG GI192M11 simulated in this study was composed of homogeny iridium 192 cylindrical core with $L = 3.5 \text{ mm}$ (length) and 0.6 mm in diameter, the density of iridium used in this work was 22.56 gcm^{-3} . The active core is surrounded by an air shell and then encapsulated in a stainless steel

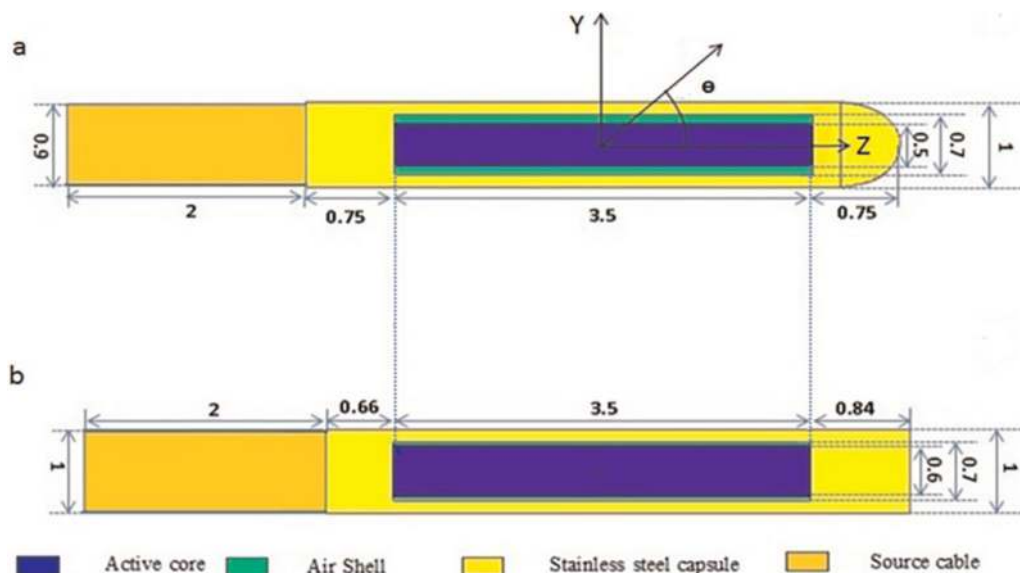


Figure 1. (a) Schematic representation for the ^{60}Co source (model: Co0.A86). (b) Schematic representation for the ^{192}Ir source (model: GI192M11) (dimensions in mm).

cylindrical capsule of 0.15 mm thick and 1 mm for the external diameter, The source cable length and diameter used in this study, we consider, are 2 mm and 1 mm, respectively, **Figure 1b**; the activity of the iridium source used in this work was $A_0 = 370\text{GBq}$, and the iridium 192 half-life is $t_{1/2} = 73.81$ days. The density used for the stainless steel is the same as used for the ^{60}Co (Co0.A86) source.

4. Monte Carlo calculations

For this work, we use the MCNPX version: 2.70 (license: C00810MNYCP) originally developed in the Los Alamos laboratory (Radiation Safety Information Computer Center, US). With the visual Editor VisedX_24E, this edition includes the package MCNP6.1/MCNP5-1.60/MCNPX-2.7.0. In addition, different tools were used for geometry modeling, particles transport, and 3D viewing of the defined geometry for the source and detectors with a dynamic model of simulation. To define the dosimetric parameters, MCNPX has different tallies to estimate each type of calculation. We consider the ^{60}Co source used this study composed of two gamma energies: 1.173 MeV and 1.332 MeV. The radiation spectrum of the ^{192}Ir source used was obtained from the database of (National Nuclear Data Center) neglecting the β spectrum for both of the simulated sources, since its contribution to the dose rate distribution is negligible due to the encapsulation [6, 16]. The Monte Carlo code fulfills all the recommendations of the report, “Dosimetric prerequisites for routine clinical use of photons emitting brachytherapy sources with average energy higher than 50 keV” of the AAPM and ESTRO. The following compilation options were used: CHEAP, DEC, PLOT, MCPLLOT, GKSSIM, XS64, CEM, INCL, HISTP, MESHTAL, RADIOG, and SPABI. The physic models of MCNPX used in this study operating the new updated photons and electrons, the photons cross sections libraries mcplib02 and mcplib84 updated from mcplib04 photon Compton broadening data for MCNP5 [17], and the el03 for electrons.

The spectrum of gamma rays used in the simulations was obtained from the (National Nuclear Data Center) [18]; we use a cutoff energy of 10 keV for both of photons and electrons. Up to 2×10^9 photon histories were simulated in this study using an Intel® Xeon (R) CPU E5620@2.40GH \times 16, HP-Z600 work station. No technique of variance reduction was used. To calculate the 2D along & away in water, the source was located in the center of a spherical phantom 40 cm in radius; acts like an unbounded phantom up to 20 cm from the source center for both ^{60}Co and ^{192}Ir sources. The density for the liquid water was 0.998 gcm^{-3} at 22°C according to the HEBD Working Group report. The coordinate axes used are shown in **Figure 1**. To obtain the radial dose function, and the along & away dose rate in the 2D Cartesian look-up table, we use a cylindrical rings system of 400×800 with 0.05 cm thick concentric to the longitudinal axis.

The high gamma energy of the ^{60}Co source takes electronic disequilibrium up to a distance of about 0.7 cm in water. Thus, we cannot approximate kerma by the dose in the near region to the source as in the case of ^{192}Ir . Consequently, the doses have been scored in distances near the source. The scored values for dose rate were included in the tables given in this study for the located points at distances where electronic disequilibrium exists. For distance greater than 1 cm from the source, to decrease the statistical uncertainty, the dose was approximate by the scored kerma; a previous study of Ballester et al., (2005) mentioned that the differences between dose and kerma are negligible at distances greater than 1 cm [19]. 10^9 Photon histories were

Element	Medium		
	Water (%)	Air (%)	Stainless steel (%)
H	11.010	0.073	—
C	—	0.012	0.03
N	—	75.032	0.01
O	88.900	—	—
Si	—	—	0.75
P	—	—	0.045
S	—	—	0.03
Ar	—	1.274	—
Cr	—	—	17.0
Mn	—	—	2.0
Fe	—	—	65.543
Ni	—	—	12.0
Mo	—	—	2.5
Co	—	—	—
Ir	—	—	—
Total mass percentage	99.910	76.391	99.908
Density (g/cm^3)	0.998	0.012	8.03

Table 1. Elemental composition used in this study by mass percentage for: sources and water phantom, (international commission on radiation units and measurements, ICRU report 44, 1989) [20].

Monte Carlo study	S_K/A ($*10^{-7}UBq^{-1}$)	Λ ($cGyh^{-1}U^{-1}$)	Source model
⁶⁰ Co			
Geant4 (Granero et al. 2007)	—	1.087 ± 0.011	BEBIG Co0.A86
EGSnrc (Anwarul et al. 2012)	3.039 ± 0.004	1.097 ± 0.001	BEBIG Co0.A86
PENELOPE (Guerrero et al. 2014)	3.046 ± 0.007	1.094 ± 0.003	BEBIG Co0.A86
EGS5 (H.Badry et al. 2018)	3.042 ± 0.007	1.092 ± 0.008	BEBIG Co0.A86
MCNPX (This work)	3.030 ± 0.002	1.092 ± 0.001	BEBIG Co0.A86
¹⁹² Ir			
Geant3 (Perez Calatayud et al. 2012)	1.091	1110	BEBIG GI192M11
Geant4 (Granero et al. 2005)	—	1.108 ± 0.003	BEBIG GI192M11
MCNPX (This work)	$1.092 \pm 0,004$	1.108 ± 0.004	BEBIG GI192M11

Table 2.

Per unite source activity and Λ , obtained with MCNPX, compared with the values obtained in other previous studies.

simulated to obtain dose rate values in the region of electronic disequilibrium and 2.10^9 photon histories to score kerma for the ⁶⁰Co source. 10^9 photon histories were used to estimate kerma for the ¹⁹²Ir source.

To investigate the air-kerma strength, we kept the source in the center of a cubic phantom with $5 \times 5 \times 5$ m³ in dimensions. Then, the air-kerma was scored at 1 m in the transversal axis of the source using 1 mm thickness cylindrical rings, concentrated from distance 99.5 cm to 100.5 cm, filled with air, with relative humidity of 40% and mass density 0.001205 g cm⁻³. In addition to that, to avoid the correction for photon attenuation and scatter in air, we have considered outside the scoring cells filled with vacuum. Elemental composition of materials used in this simulation is shown in **Table 1**, taken from the (ICRU 44 report) [20].

The dose rate constant was calculated using Eq. (2), by dividing the scored value of dose in a cubic voxel, with $0.1 \times 0.1 \times 0.1$ mm³ in dimensions by the air-kerma strength. Therefore, the scoring zone located in 1 cm from the active core center in the transversal axis (Y-axis), in a spherical phantom of 40 cm in radius filled with water.

$$\Lambda = \frac{\dot{D}(r, \theta)}{S_k} \quad (2)$$

The values of \dot{D} and Λ were compared with the published data and presented in **Table 2**.

5. Air kerma strength

The TG-43 formalism and the full report for the HEBD Working Group of the AAPM and ESTRO recommend for HDR brachytherapy specifying photon-emitting sources in terms of the air-kerma strength S_K , taking into account correction for attenuation and scattering in air. The relation between S_K and K_{air} is given by Eq. (3) [21]:

$$S_K = K_{air}_{dref} \times d_{ref}^2 \quad (3)$$

Where the reference air-kerma rate is defined at $d_{ref} = 1$ m.

The air-kerma per source photon depends to the photon fluence by the equation:

$$K_{air} = 1.602 \cdot 10^{-10} * \int_{E_{min}}^{E_{max}} \phi(E) E \left(\frac{\mu_{en}(E)}{\rho} \right) dE \quad (4)$$

Where K_{air} is air kerma per source photon in Gy, the factor $1.602 \cdot 10^{-10}$ converted the result from MeV g^{-1} into Gy, photon fluence (cm^{-2}) at the energy E (MeV) per initial source photon at the distance d , and the mass-energy absorption coefficient ($\text{cm}^{-2} \text{g}^{-1}$) at the energy E [22].

To obtain the total air-kerma, we use the following Eq. (8) [22].

$$K_{air} = 1.602 \cdot 10^{-10} * \sum_{E_{min}}^{E_{max}} \phi(E_i) E_i \left(\frac{\mu_{en}(E_i)}{\rho} \right) \Delta E \quad (5)$$

The total air-kerma per incident photon, E_i the midpoint for an energy bin, ΔE the bin size in MeV, for this study we use the photon fluence spectrum in 10 keV intervals. Thus, we introduce the Eq. (5) by using the MCNPX F6 tally, which is a track-length estimator [23], providing results in (MeV/g) [10, 24], converted into Gy by using the appropriate FM card tally multiplier ($\text{FM} = 1.60210^{-10}$). The composition for air is taken from the tables of X-ray mass attenuation coefficients and mass energy-absorption coefficients (NIST) [25]. The HEBD recommended a short-hand notation for the air-kerma strength: $1 \text{ U} = 1 \mu\text{Gym}^2 \text{ h}^{-1} = 1 \text{ cGycm}^2 \text{ h}^{-1}$. Then to calculate the air-kerma strength per unit of source activity in $(\text{Gym}^2 \text{ s}^{-1} \text{ Bq}^{-1})$, we use Eq. (6) below:

$$\frac{Sk}{A} = K_{air}(d_{ref}) d_{ref}^2 N \quad (6)$$

Where A is the source activity (Bq) and N the number of photons per decay, considered equal 2 for the ^{60}Co source, and 2.21 for the ^{192}Ir source.

6. Radial dose function

The radial dose function $g_L(r)$ described in the protocol of the (HEBD) takes into account scattering and absorption in the transversal axis of the source; it was calculated in a spherical phantom filled with water using concentric cylindrical rings to the longitudinal axis, with 0.05 cm thickness for the ranging distance from 0.25 cm to 20 cm for both of the simulated sources in this study. The results obtained are presented in **Table 3**.

7. Along & away absorbed dose

The along & away absorbed dose rates were investigated for the ranging distance from 0.25 cm to 7 cm in the transversal axis and from 0 cm to ± 7 cm in the longitudinal axis. The 2D along & away was compared with the published data. The results

Radial distance r (cm)	g _L (r)	
	BEBIG Co0.A86 ⁶⁰ Co	BEBIG GI192M11 ¹⁹² Ir
0.25	1.0705 ± 0.0041	0.9943 ± 0.0002
0.5	1.0221 ± 0.0046	0.9987 ± 0.0002
0.75	0.9938 ± 0.0048	0.9990 ± 0.0003
1	1 ± 0.0002	1 ± 0.0003
1.5	0.9926 ± 0.0002	1.0037 ± 0.0004
2	0.9874 ± 0.0002	1.0090 ± 0.0004
3	0.9689 ± 0.0003	1.0086 ± 0.0005
4	0.9539 ± 0.0003	1.0088 ± 0.0006
5	0.9378 ± 0.0003	1.0052 ± 0.0007
6	0.9205 ± 0.0003	0.9974 ± 0.0007
7	0.9035 ± 0.0003	0.9874 ± 0.0008
8	0.8867 ± 0.0003	0.9748 ± 0.0008
9	0.8683 ± 0.0003	0.9593 ± 0.0009
10	0.8513 ± 0.0003	0.9418 ± 0.0009
12	0.8156 ± 0.0003	0.9011 ± 0.0010
15	0.7593 ± 0.0003	0.8272 ± 0.0011
20	0.6628 ± 0.0003	0.6870 ± 0.0014

Table 3.
Radial dose function obtained for ⁶⁰Co and ¹⁹²Ir using MCNPX in a water.

are tabulated in the form recommended by the HEBD Working Group report [1], **Tables 4** and **5**, respectively, for ⁶⁰Co and ¹⁹²Ir.

8. Uncertainties

The uncertainties evaluated in this study are the type A (k = 1) statistical uncertainty contribution dependent on the Monte Carlo technique. No technique of the variance reduction was used as mentioned before. All MCNPX results are normalized to be per initial particle history printed in the output with an additional number beside, which is the estimated statistical uncertainty. In this work statistical uncertainties are less than 0.8% and 0.4% type A uncertainty (k = 1) respectively for ⁶⁰Co and ¹⁹²Ir, derived by considering the contribution of the different simulated parameters for both of the simulated sources. In addition to the contribution of the propagated uncertainty for both of radial dose function and the 2D along & away in the relative uncertainties of the MCNPX output tallies. For the cobalt source dose rates, uncertainties were calculated from the quadrature sum of uncertainties obtained for the dose scored in the near distance to the source, and the scored kerma for the distance where the electronic equilibrium is reached.

Type B uncertainties are difficult to evaluate because of different contributions such as uncertainties of the cross section and energy spectrum, uncertainties in the modeled geometry of the source, and uncertainties in the scoring dose and kerma

Distance along Z-axis (cm)	Distance away in Y-Axis (cm)													
	0.25	0.5	0.75	1	1.5	2	3	4	5	6	7			
-7	0.0189 ± 0.0109	0.0172 ± 0.0103	0.0206 ± 0.0099	0.0187 ± 0.0026	0.0187 ± 0.0022	0.0182 ± 0.0021	0.0168 ± 0.0021	0.0149 ± 0.0021	0.0130 ± 0.0021	0.0112 ± 0.0020	0.0096 ± 0.0020			
-6	0.0220 ± 0.0105	0.0213 ± 0.0097	0.0295 ± 0.0093	0.0259 ± 0.0024	0.0257 ± 0.0022	0.0247 ± 0.0021	0.0220 ± 0.0021	0.0190 ± 0.0021	0.0160 ± 0.0021	0.0134 ± 0.0020	0.0112 ± 0.0020			
-5	0.0350 ± 0.0101	0.0406 ± 0.0091	0.0392 ± 0.0088	0.0381 ± 0.0023	0.0369 ± 0.0021	0.0350 ± 0.0021	0.0297 ± 0.0020	0.0245 ± 0.0020	0.0199 ± 0.0020	0.0160 ± 0.0020	0.0130 ± 0.0020			
-4	0.0668 ± 0.0091	0.0613 ± 0.0086	0.0608 ± 0.0085	0.0597 ± 0.0022	0.0564 ± 0.0021	0.0516 ± 0.0020	0.0412 ± 0.0020	0.0319 ± 0.0020	0.0245 ± 0.0020	0.0190 ± 0.0020	0.0150 ± 0.0020			
-3	0.1092 ± 0.0087	0.1099 ± 0.0083	0.1044 ± 0.0081	0.1045 ± 0.0021	0.0995 ± 0.0020	0.0811 ± 0.0020	0.0581 ± 0.0020	0.0412 ± 0.0020	0.0300 ± 0.0020	0.0222 ± 0.0020	0.0169 ± 0.0020			
-2	0.2578 ± 0.0081	0.2640 ± 0.0078	0.2515 ± 0.0075	0.2149 ± 0.0021	0.1716 ± 0.0020	0.1340 ± 0.0020	0.0811 ± 0.0020	0.0521 ± 0.0020	0.0355 ± 0.0020	0.0252 ± 0.0020	0.0187 ± 0.0020			
-1.5	0.4886 ± 0.0075	0.4445 ± 0.0073	0.3886 ± 0.0070	0.3355 ± 0.0020	0.2403 ± 0.0020	0.1725 ± 0.0020	0.0942 ± 0.0020	0.0573 ± 0.0020	0.0378 ± 0.0020	0.0264 ± 0.0020	0.0194 ± 0.0020			
-1	1.0378 ± 0.0072	0.8976 ± 0.0068	0.7078 ± 0.0066	0.5473 ± 0.0020	0.3355 ± 0.0020	0.2163 ± 0.0020	0.1064 ± 0.0020	0.0616 ± 0.0020	0.0397 ± 0.0020	0.0274 ± 0.0020	0.0199 ± 0.0020			
-0.75	1.8579 ± 0.0068	1.3801 ± 0.0066	0.9897 ± 0.0064	0.7019 ± 0.0020	0.3878 ± 0.0020	0.2375 ± 0.0020	0.1114 ± 0.0020	0.0633 ± 0.0020	0.0404 ± 0.0020	0.0276 ± 0.0020	0.0201 ± 0.0020			
-0.5	3.8827 ± 0.0060	2.3749 ± 0.0062	1.4126 ± 0.0063	0.8780 ± 0.0020	0.4354 ± 0.0020	0.2546 ± 0.0020	0.1152 ± 0.0020	0.0645 ± 0.0020	0.0409 ± 0.0020	0.0278 ± 0.0020	0.0202 ± 0.0020			
-0.25	10.1078 ± 0.0047	3.6613 ± 0.0059	1.7678 ± 0.0061	1.0279 ± 0.0020	0.4711 ± 0.0020	0.2665 ± 0.0020	0.1178 ± 0.0020	0.0654 ± 0.0020	0.0412 ± 0.0020	0.0281 ± 0.0020	0.0203 ± 0.0020			
0	16.9827 ± 0.0041	4.4647 ± 0.0046	1.9732 ± 0.0048	1.0898 ± 0.0020	0.4830 ± 0.0020	0.2713 ± 0.0020	0.1185 ± 0.0020	0.0657 ± 0.0020	0.0414 ± 0.0020	0.0281 ± 0.0020	0.0203 ± 0.0020			
0.25	10.0821 ± 0.0044	3.6851 ± 0.0050	1.8212 ± 0.0053	1.0279 ± 0.0020	0.4711 ± 0.0020	0.2665 ± 0.0020	0.1175 ± 0.0020	0.0654 ± 0.0020	0.0412 ± 0.0020	0.0281 ± 0.0020	0.0203 ± 0.0020			
0.5	4.0092 ± 0.0047	2.2930 ± 0.0054	1.3918 ± 0.0055	0.8780 ± 0.0020	0.4354 ± 0.0020	0.2546 ± 0.0020	0.1152 ± 0.0020	0.0647 ± 0.0020	0.0409 ± 0.0020	0.0278 ± 0.0020	0.0202 ± 0.0020			
0.75	1.8878 ± 0.0059	1.3874 ± 0.0059	1.0309 ± 0.0057	0.7019 ± 0.0020	0.3878 ± 0.0020	0.2375 ± 0.0020	0.1114 ± 0.0020	0.0633 ± 0.0020	0.0404 ± 0.0020	0.0276 ± 0.0020	0.0201 ± 0.0020			
1	1.0680 ± 0.0067	0.8909 ± 0.0064	0.7267 ± 0.0062	0.5473 ± 0.0020	0.3355 ± 0.0020	0.2165 ± 0.0020	0.1064 ± 0.0020	0.0616 ± 0.0020	0.0397 ± 0.0020	0.0274 ± 0.0020	0.0199 ± 0.0020			
1.5	0.4672 ± 0.0071	0.4276 ± 0.0069	0.3945 ± 0.0066	0.3355 ± 0.0020	0.2403 ± 0.0020	0.1725 ± 0.0020	0.0942 ± 0.0020	0.0573 ± 0.0020	0.0378 ± 0.0020	0.0264 ± 0.0020	0.0194 ± 0.0020			
2	0.2684 ± 0.0078	0.2406 ± 0.0072	0.2382 ± 0.0070	0.2146 ± 0.0021	0.1716 ± 0.0020	0.1340 ± 0.0020	0.0811 ± 0.0020	0.0521 ± 0.0020	0.0355 ± 0.0020	0.0252 ± 0.0020	0.0187 ± 0.0020			
3	0.1211 ± 0.0083	0.1093 ± 0.0077	0.1053 ± 0.0074	0.1049 ± 0.0021	0.0937 ± 0.0021	0.0811 ± 0.0021	0.0578 ± 0.0020	0.0412 ± 0.0020	0.0300 ± 0.0020	0.0222 ± 0.0020	0.0169 ± 0.0020			
4	0.0593 ± 0.0088	0.0630 ± 0.0081	0.0603 ± 0.0078	0.0602 ± 0.0022	0.0564 ± 0.0021	0.0519 ± 0.0021	0.0412 ± 0.0021	0.0319 ± 0.0021	0.0245 ± 0.0021	0.0191 ± 0.0020	0.0150 ± 0.0020			
5	0.0315 ± 0.0093	0.0381 ± 0.0087	0.0379 ± 0.0081	0.0385 ± 0.0023	0.0371 ± 0.0021	0.0350 ± 0.0021	0.0297 ± 0.0021	0.0245 ± 0.0021	0.0198 ± 0.0021	0.0160 ± 0.0020	0.0130 ± 0.0020			
6	0.0221 ± 0.0100	0.00295 ± 0.0093	0.0215 ± 0.0091	0.0264 ± 0.0024	0.0257 ± 0.0022	0.0247 ± 0.0022	0.0221 ± 0.0021	0.0190 ± 0.0021	0.0160 ± 0.0021	0.0134 ± 0.0020	0.0112 ± 0.0020			
7	0.0176 ± 0.0104	0.0192 ± 0.0101	0.0187 ± 0.0098	0.0192 ± 0.0026	0.0189 ± 0.0022	0.0184 ± 0.0022	0.0168 ± 0.0021	0.0149 ± 0.0021	0.0130 ± 0.0021	0.0112 ± 0.0020	0.0096 ± 0.0020			

Table 4. Dose rate along \hat{x} away per unit air-kerma strength ($\text{cGy h}^{-1} \text{U}^{-1}$) in liquid water obtained for the BEBIG ^{60}Co source (model: Coo.A86), (+Z toward the source tip and -Z toward the delivery cable).

Distance along Z-axis (cm)	Distance away in Y-axis (cm)													
	0.25	0.5	0.75	1	1.5	2	3	4	5	6	7			
-7	0.0158 ± 0.0047	0.016 ± 0.0033	0.0164 ± 0.0027	0.0170 ± 0.0023	0.0174 ± 0.0019	0.0176 ± 0.0016	0.0169 ± 0.0013	0.0155 ± 0.0012	0.0137 ± 0.0011	0.0120 ± 0.0011	0.0103 ± 0.0011			
-6	0.0210 ± 0.0042	0.0218 ± 0.0029	0.0225 ± 0.0024	0.0232 ± 0.0020	0.0240 ± 0.0016	0.0239 ± 0.0014	0.0223 ± 0.0012	0.0198 ± 0.0011	0.0171 ± 0.0010	0.0144 ± 0.0010	0.0122 ± 0.0010			
-5	0.0297 ± 0.0036	0.0311 ± 0.0025	0.0326 ± 0.0020	0.0338 ± 0.0017	0.0345 ± 0.0014	0.0340 ± 0.0012	0.0302 ± 0.0010	0.0256 ± 0.0010	0.0212 ± 0.0009	0.0173 ± 0.0009	0.0142 ± 0.0010			
-4	0.0455 ± 0.0030	0.0488 ± 0.0020	0.0516 ± 0.0016	0.0533 ± 0.0014	0.0533 ± 0.0011	0.0507 ± 0.0010	0.0422 ± 0.0009	0.0335 ± 0.0009	0.0263 ± 0.0009	0.0207 ± 0.0009	0.0164 ± 0.0009			
-3	0.0800 ± 0.0023	0.0884 ± 0.0015	0.0935 ± 0.0012	0.0944 ± 0.0011	0.0897 ± 0.0009	0.0805 ± 0.0008	0.0599 ± 0.0008	0.0437 ± 0.0008	0.0321 ± 0.0008	0.0242 ± 0.0008	0.0186 ± 0.0008			
-2	0.1839 ± 0.0015	0.2069 ± 0.0010	0.2100 ± 0.0008	0.2007 ± 0.0007	0.1688 ± 0.0007	0.1353 ± 0.0006	0.0846 ± 0.0006	0.0554 ± 0.0007	0.0381 ± 0.0007	0.0275 ± 0.0008	0.0206 ± 0.0008			
-1.5	0.3408 ± 0.0012	0.3736 ± 0.0008	0.3563 ± 0.0006	0.3201 ± 0.0006	0.2394 ± 0.0006	0.1756 ± 0.0006	0.0987 ± 0.0006	0.0610 ± 0.0006	0.0408 ± 0.0007	0.0288 ± 0.0007	0.0213 ± 0.0008			
-1	0.8279 ± 0.0007	0.8053 ± 0.0005	0.6747 ± 0.0005	0.5376 ± 0.0005	0.3374 ± 0.0005	0.2220 ± 0.0005	0.1116 ± 0.0006	0.0658 ± 0.0006	0.0429 ± 0.0007	0.0299 ± 0.0007	0.0219 ± 0.0008			
-0.75	1.5283 ± 0.0005	1.2924 ± 0.0004	0.9574 ± 0.0004	0.6973 ± 0.0004	0.3921 ± 0.0004	0.2441 ± 0.0005	0.1168 ± 0.0005	0.0675 ± 0.0006	0.0437 ± 0.0007	0.0303 ± 0.0007	0.0221 ± 0.0008			
-0.5	3.4028 ± 0.0004	2.1718 ± 0.0003	1.3443 ± 0.0003	0.8780 ± 0.0004	0.4429 ± 0.0004	0.2626 ± 0.0005	0.1208 ± 0.0005	0.0689 ± 0.0006	0.0442 ± 0.0007	0.0305 ± 0.0007	0.0222 ± 0.0008			
-0.25	9.1268 ± 0.0002	3.4770 ± 0.0003	1.7488 ± 0.0003	1.0360 ± 0.0003	0.4798 ± 0.0004	0.2750 ± 0.0004	0.1234 ± 0.0004	0.0696 ± 0.0005	0.0445 ± 0.0006	0.0307 ± 0.0007	0.0224 ± 0.0007			
0	15.4135 ± 0.0002	4.2627 ± 0.0002	1.9391 ± 0.0003	1.1005 ± 0.0003	0.4937 ± 0.0004	0.2796 ± 0.0004	0.1244 ± 0.0005	0.0700 ± 0.0006	0.0446 ± 0.0007	0.0307 ± 0.0007	0.0224 ± 0.0008			
0.25	9.1199 ± 0.0002	3.4777 ± 0.0003	1.7498 ± 0.0003	1.0352 ± 0.0003	0.4801 ± 0.0004	0.2750 ± 0.0004	0.1234 ± 0.0005	0.0697 ± 0.0006	0.0445 ± 0.0007	0.0307 ± 0.0007	0.0223 ± 0.0008			
0.5	3.3981 ± 0.0004	2.1709 ± 0.0003	1.3443 ± 0.0003	0.8782 ± 0.0004	0.4430 ± 0.0004	0.2627 ± 0.0005	0.1209 ± 0.0005	0.0690 ± 0.0006	0.0442 ± 0.0007	0.0305 ± 0.0007	0.0223 ± 0.0008			
0.75	1.5284 ± 0.0005	1.2915 ± 0.0004	0.9570 ± 0.0004	0.6970 ± 0.0004	0.3921 ± 0.0004	0.2442 ± 0.0005	0.1168 ± 0.0005	0.0675 ± 0.0006	0.0437 ± 0.0007	0.0303 ± 0.0007	0.0221 ± 0.0008			
1	0.8355 ± 0.0007	0.8050 ± 0.0005	0.6741 ± 0.0005	0.5373 ± 0.0005	0.3373 ± 0.0005	0.2217 ± 0.0005	0.1114 ± 0.0006	0.0657 ± 0.0006	0.0429 ± 0.0007	0.0299 ± 0.0007	0.0219 ± 0.0008			
1.5	0.3519 ± 0.0011	0.3735 ± 0.0008	0.3561 ± 0.0006	0.3198 ± 0.0006	0.2394 ± 0.0006	0.1755 ± 0.0006	0.0985 ± 0.0006	0.0610 ± 0.0006	0.0408 ± 0.0007	0.0289 ± 0.0007	0.0213 ± 0.0008			
2	0.1931 ± 0.0015	0.2090 ± 0.0010	0.2101 ± 0.0008	0.2006 ± 0.0007	0.1687 ± 0.0007	0.1352 ± 0.0006	0.0847 ± 0.0006	0.0554 ± 0.0007	0.0381 ± 0.0007	0.0275 ± 0.0008	0.0205 ± 0.0008			
3	0.0857 ± 0.0022	0.0910 ± 0.0015	0.0943 ± 0.0012	0.0947 ± 0.0011	0.0898 ± 0.0009	0.0805 ± 0.0008	0.0598 ± 0.0008	0.0436 ± 0.0008	0.0322 ± 0.0008	0.0242 ± 0.0008	0.0186 ± 0.0008			
4	0.0488 ± 0.0029	0.0506 ± 0.0020	0.0527 ± 0.0016	0.0537 ± 0.0014	0.0534 ± 0.0011	0.0508 ± 0.0010	0.0422 ± 0.0009	0.0335 ± 0.0009	0.0263 ± 0.0009	0.0207 ± 0.0009	0.0164 ± 0.0009			
5	0.0316 ± 0.0035	0.0325 ± 0.0024	0.0336 ± 0.0020	0.0342 ± 0.0017	0.0347 ± 0.0014	0.0340 ± 0.0012	0.0303 ± 0.0010	0.0256 ± 0.0010	0.0212 ± 0.0009	0.0174 ± 0.0009	0.0142 ± 0.0010			
6	0.0222 ± 0.0041	0.0228 ± 0.0029	0.0232 ± 0.0023	0.0236 ± 0.0020	0.0241 ± 0.0016	0.0240 ± 0.0014	0.0223 ± 0.0012	0.0198 ± 0.0011	0.0170 ± 0.0010	0.0144 ± 0.0010	0.0122 ± 0.0010			
7	0.0165 ± 0.0047	0.0168 ± 0.0033	0.0170 ± 0.0027	0.0174 ± 0.0023	0.0177 ± 0.0019	0.0177 ± 0.0016	0.0169 ± 0.0013	0.0155 ± 0.0012	0.0138 ± 0.0011	0.0120 ± 0.0011	0.0103 ± 0.0011			

Table 5. Dose rate along \hat{e}_r away per unit air-kerma strength ($cGy h^{-1} U^{-1}$) in liquid water for the BEBIG ^{192}Ir source (model: G1192M11), ($+Z$ toward the source tip and $-Z$ toward the delivery cable).

process. Thus we considered type B uncertainty negligible, and we reduced the uncertainty to statistical uncertainty. A description of the methodology used to estimate the type B uncertainties is mentioned in the updated report of the TG-43 [21] and the HEBD working group report [1].

9. Results and discussion

Table 2 illustrates the results obtained in this study for both the air-kerma strength and the dose rate constant for the two studied sources compared with the quoted results in previous studies. The value calculated for the air-kerma strength for the ^{60}Co source was 3.030 ± 0.002 (10^{-7} U Bq $^{-1}$), this value agrees well with the value 3.039 ± 0.004 ($*10^{-7}$ U Bq $^{-1}$) obtained by (Anwarul et al., 2012) in their study [4]. Also, H. Badry et al., (2018) obtained the value 3.042 ± 0.007 ($*10^{-7}$ U Bq $^{-1}$) in their work [5], and Guerrero et al., (2014) found the value 3.046 ± 0.0070 ($*10^{-7}$ U Bq $^{-1}$) with a maximum difference of 1.6%. For the ^{192}Ir source [3], the value obtained for the air-kerma strength, which is 1.092 ± 0.004 ($*10^{-7}$ U Bq $^{-1}$), was compared with the available quoted value from Perez-Calatayud et al., (2012) [1], the difference was within 0.1%.

For the constant of dose rate, we found for the ^{60}Co a value of 1.092 ± 0.001 cGy h $^{-1}$ U $^{-1}$. This result was compared with the published data quoted in **Table 2**, and we found a maximum difference of 0.5% with Granero et al. (2007) and Anwarul et al., (2012) [2, 4]. The result found for the ^{192}Ir source was 1.109 ± 0.004 cGy h $^{-1}$ U $^{-1}$, compared with the published data we found a maximum difference of 0.1% with the results obtained by Perez-Calatayud et al., (2012) and Granero et al. (2005) in their work [1, 6].

The radial dose function obtained for the ^{60}Co source in this work (**Table 3**) was in good agreement with the obtained results in other studies using different Monte Carlo codes, especially, for distances (>1 cm) (**Figure 2a**). The **Figure 2b** represented the ratio $g_L(r)_{\text{reference}}/g_L(r)_{\text{this work}}$ calculated to evaluate the deviation of our results from the published data. We observe for the distance greater than 1 cm a maximum relative difference of 0.94% compared with H. Badry et al., (2018) [5]. For the near distance to the source, a maximum relative difference of 6% was found compared with Guerrero et al., (2014) [3], 2.14% compared with H. Badry et al., (2018) [5], and 1.65% compared with Granero et al., (2007) [2]. These results can be attributed partially to the variety of the physics models for radiation transport used in each Monte Carlo code, on the one hand. On the other hand, it can be assigned to the differences in simulated geometries impact. For the ^{192}Ir source (G1192M11), the obtained radial dose function in this work using MCNPX is presented in **Figure 3a**. The comparison with previous works, for the range of distance from 0.25 to 20 cm, was performed using the expression $g_L(r)_{\text{reference}}/g_L(r)_{\text{this work}}$ presented in the **Figure 3b**. For the distance near to the source, we observe a maximum relative difference of 0.40% compared with D. Granero et al., (2005) [6]. For distances greater than 1 cm, the maximum relative difference found was 0.74%. The comparison in the case of the ^{192}Ir was also made with the results obtained for the BEBIG Ir2. A852 source model. The maximum difference was found to be within 1.51% compared with D. Granero et al., (2008) [7] and 0.50% if the comparison is made with Belousov et al., (2014) [8].

The radial dose functions investigated using MCNPX for both ^{60}Co and ^{192}Ir were compared between each other by calculating the ratio $g_L(r)_{\text{Co-60}}/g_L(r)_{\text{Ir-192}}$ illustrated

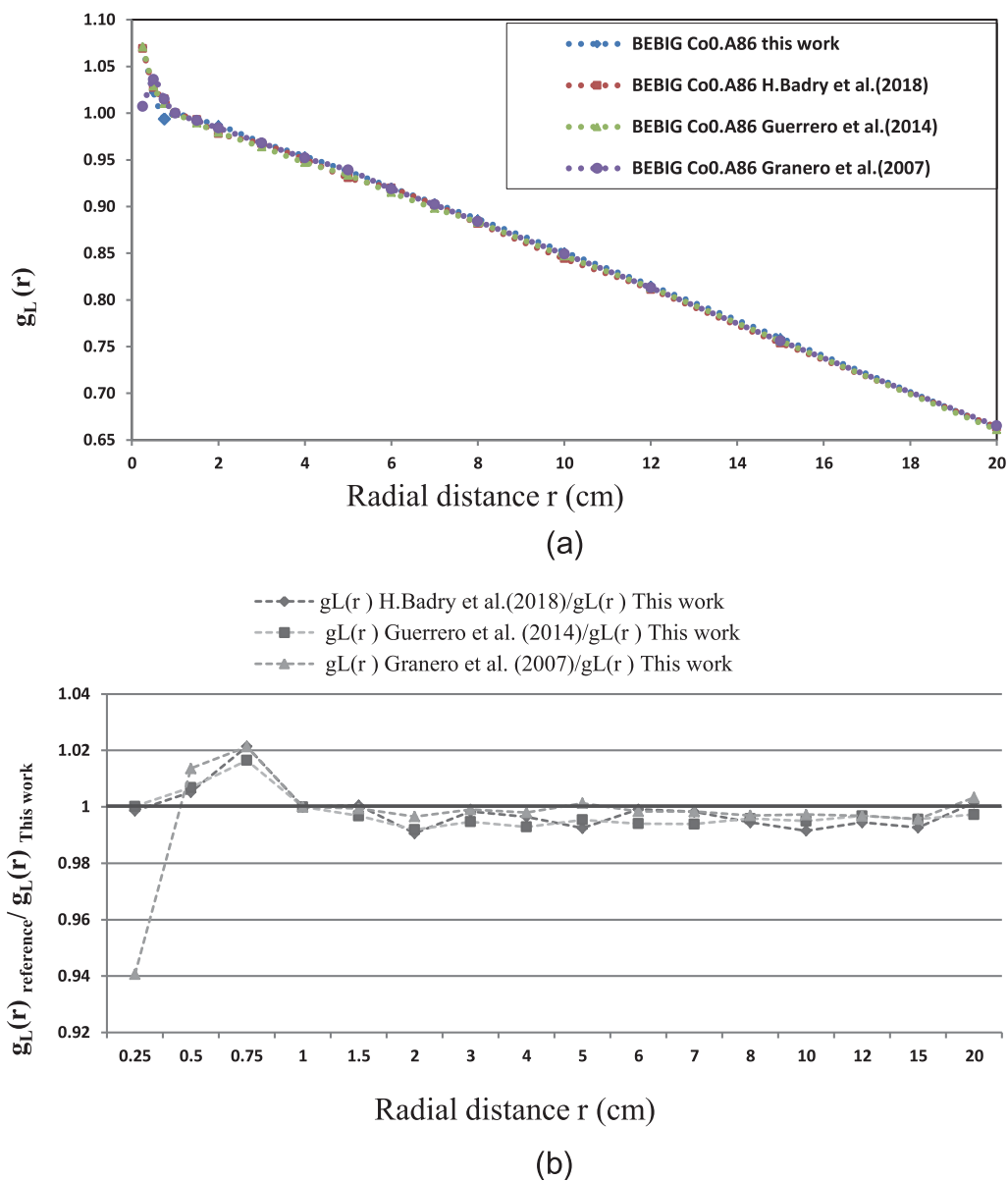
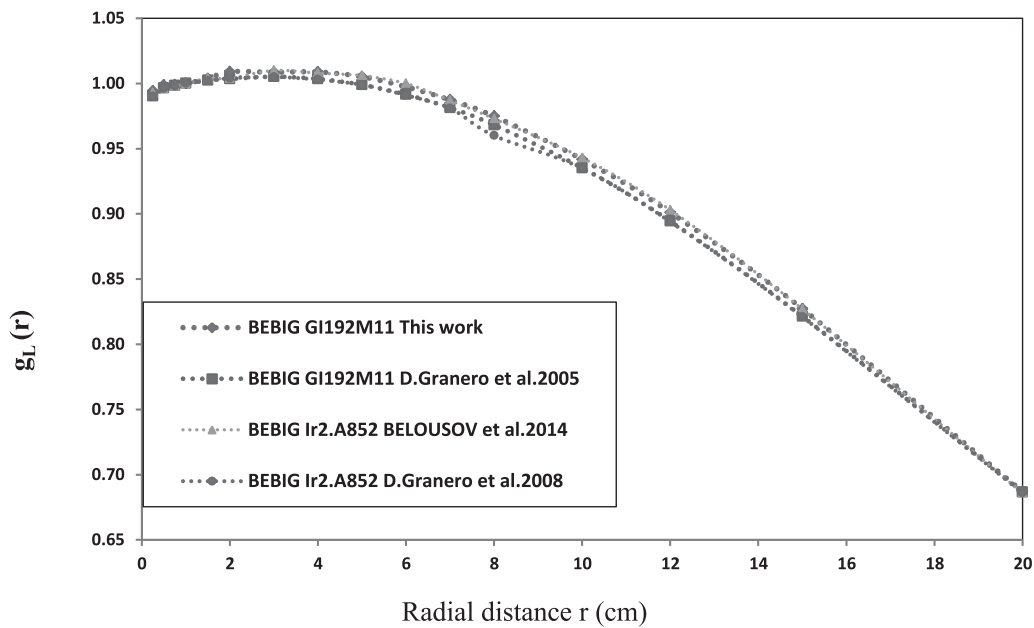


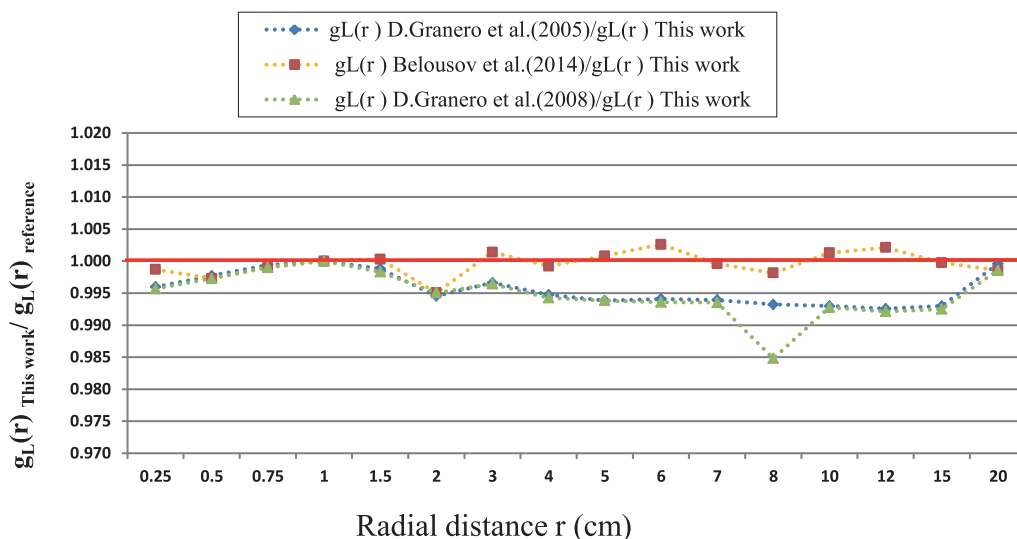
Figure 2.
 (a) The curve of radial dose function for ^{60}Co (Coo.A86) obtained with MCNPX compared with the published data for the same model source. (b) The curves of ratio $g_L(r)_{\text{This work}}/g_L(r)_{\text{reference}}$ for ^{60}Co (Coo.A86) obtained with MCNPX compared with previous studies for the same source model.

in **Figure 4**. We observe that the radial dose function calculated for ^{60}Co decrease faster than the ^{192}Ir radial dose function. This difference between the two radial dose functions reached 10% for the distance of 9 cm. This makes the absorbed dose around the two sources different. In addition, regarding the slow decreases of radial dose function for the ^{192}Ir source, we conclude that the ^{192}Ir source could deliver a bit overdoses to the organs at risk more than the ^{60}Co source, especially for tumors of high dimensions in gynecological applications.

The 2D along & away dose rates per unit of air-kerma strength were investigated for the BEBIG ^{60}Co and ^{192}Ir using the same geometry of detectors as mentioned before. The results obtained are tabulated (**Tables 4 and 5**), compared with the



(a)



(b)

Figure 3.
 (a) The curve of radial dose function for ^{192}Ir (GI192M11) obtained with MCNPX compared with the available published data. (b) The curves of ratio $g_L(r)_{\text{This work}}/g_L(r)_{\text{reference}}$ for ^{192}Ir (GI192M11) obtained with MCNPX compared with the previous studies for the same source model, and the source model Ir2.A852.

published data, the results are in good consistency. A comparison was made for the maximum dose rate per U, located in the distance 0.25 cm away in the transversal axis. For the BEBIG ^{60}Co source, we obtain a maximum dose rate per U, which is $16.98 \text{ cGy h}^{-1} \text{ U}^{-1}$ agreeing well with value found by H. Badry et al., (2018) [5], which is $16.55 \text{ cGy h}^{-1} \text{ U}^{-1}$. Furthermore, Granero et al., (2007) [2] found a value of $15.15 \text{ cGy h}^{-1} \text{ U}^{-1}$. Otherwise, For the BEBIG ^{192}Ir source, we found a value of $15.41 \text{ cGy h}^{-1} \text{ U}^{-1}$ in this study, and Granero et al., (2005) [6] obtained

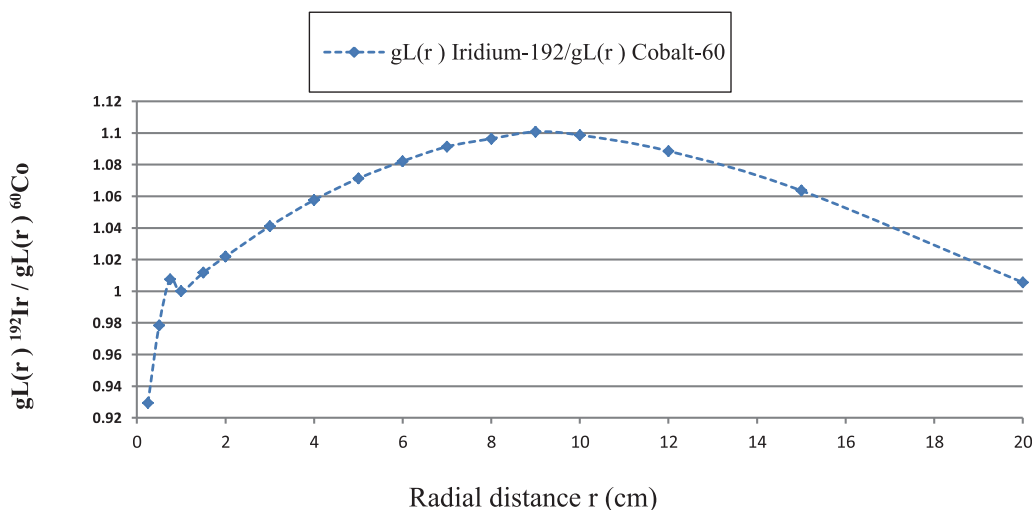


Figure 4. The curve of the ratio $g_L(r)_{192Ir}/g_L(r)_{Co-60}$, calculated to compare the differences between the results obtained for $g_L(r)$ for both sources Co0.A86 and G1192M11.

15.50 cGy h⁻¹ U⁻¹ in their work for the same model. Moreover, Granero et al., (2006) [26] found in their study for Flexisource ¹⁹²Ir HDR source model a value of 15.56 cGy h⁻¹ U⁻¹. Also E. Reys et al., (2016) found 15.57 cGy h⁻¹ U⁻¹ in their work for the GammaMed HDR Plus ¹⁹²Ir source model [24].

For the comparison made between the results obtained in this work for both BEBIG sources, we observe that the generated 2D along & away dose rates per unit of air-kerma strength for the near distance to the source are greater for the ⁶⁰Co than for ¹⁹²Ir. On the contrary, for distances greater than 1 cm, we observe that the values calculated for the ¹⁹²Ir source are a little greater than for ⁶⁰Co source, this difference increases by increasing the distance away in the transversal axis, **Figure 5**. Regarding the contribution of different dosimetric parameters in the treatment planning systems, this difference can be considered negligible within the agreement, concerning the clinic practice for the treated volume [12].

Outside of the treated volume, a study made by Venselaar et al. (1996) mentioned that the absorbed dose in peripheral organs at risk showed opposite behavior (¹⁹²Ir doses > ⁶⁰Co doses) at distances near the treated volume in contrast to the behavior (¹⁹²Ir doses < ⁶⁰Co doses) at larger distances [13]. In addition, recent study of dose delivered to organs has been calculated on a reference male phantom for a typical implant of the prostate in HDR brachytherapy using Monte Carlo method [14]. For the closest organs, equivalent delivered doses by ⁶⁰Co were less (8–19%) than for ¹⁹²Ir. However, increasing the distance beyond 10 cm, high equivalent doses were delivered by ⁶⁰Co. The overall result is that effective doses per clinical absorbed dose from a ¹⁹²Ir source are about 18% greater than from a ⁶⁰Co source [14].

10. Conclusion

In conclusion, the minor differences on the absorbed dose around the two sources observed in the radial dose function decrease and the 2D along & away dose rate per unit of air-kerma strength. For ⁶⁰Co and ¹⁹²Ir is considered negligible within the agreement by the specialists evaluated the use of ⁶⁰Co in the afterloading devices as

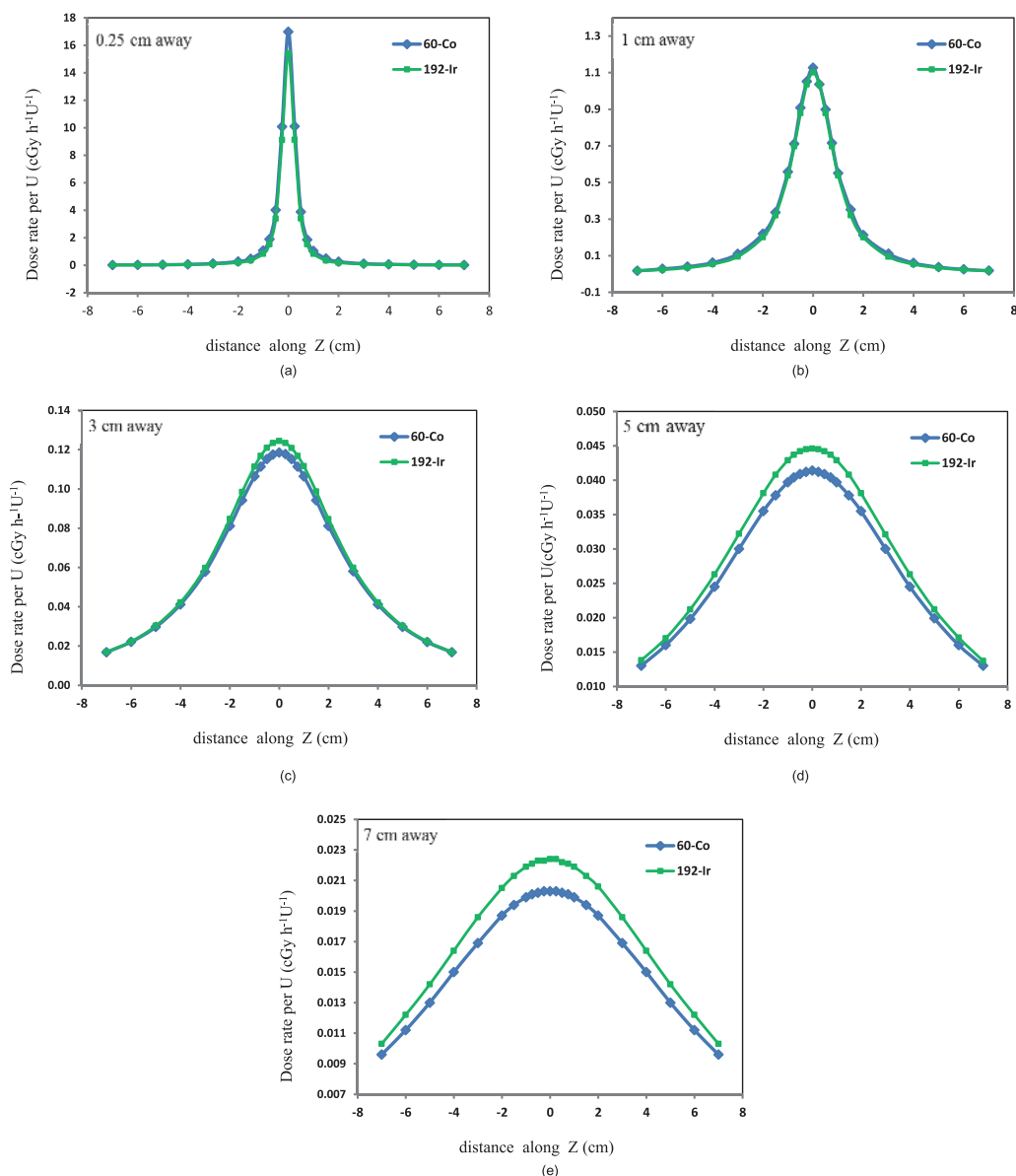


Figure 5. A comparison between dose rate per unit of air-kerma strength of ^{60}Co (Coo.A86) and ^{192}Ir (GI192M11) sources in different away distances ($a = 0.25\text{ cm}$, $b = 1\text{ cm}$, $c = 3\text{ cm}$, $d = 5\text{ cm}$, $e = 7\text{ cm}$).

^{192}Ir equivalent. Their studies show that there are no significant differences between the two sources concerning the prescribing dose in a typical brachytherapy applications, neither in the treatment planning nor isodose distributions to target on the one hand. On the other hand, economic aspects make the ^{60}Co an important option for clinics over the world. The recent introduction of miniaturized ^{60}Co sources by Eckert & Ziegler BEBIG is considered as a mutation for this nuclide in HDR brachytherapy. The previous study announced that ^{60}Co sources have potential logistical advantages and replacement intervals due to decay. One exchange of the ^{60}Co source required 25 source exchanges for ^{192}Ir , and this reduced operating costs, and makes ^{60}Co a good option to be considered for applications in brachytherapy HDR, especially for the developing countries.

Author details

Said Elboukhari^{1*}, Khalid Yamni¹, Hmad Ouabi², Taoufiq Bouassa³
and Lahcen Ait Mlouk⁴

1 Faculty of Sciences, EMaMePS, Department of Chemistry, Moly Ismail University of Meknes, Morocco


2 Center of Oncology ALAZHAR, Rabat, Morocco

3 Faculty of Sciences, Mohammed V University of Rabat, Morocco

4 Faculty of Sciences, Moly Ismail University of Meknes, Morocco

*Address all correspondence to: saidhorion@gmail.com

IntechOpen

© 2022 The Author(s). Licensee IntechOpen. This chapter is distributed under the terms of the Creative Commons Attribution License (<http://creativecommons.org/licenses/by/3.0>), which permits unrestricted use, distribution, and reproduction in any medium, provided the original work is properly cited. 

References

- [1] Perez-Calatayud J, Ballester F, Das RK, Dewerd LA, Ibbott GS, Meigooni AS, et al. Dose calculation for photon-emitting brachytherapy sources with average energy higher than 50 keV: (HEBD) Working Group report of the AAPM and ESTRO. *Medical Physics*. 2012;**39**(5):2904-2929. DOI: 10.1118/1.3703892
- [2] Granero D, Pérez-Calatayud J, Ballester F. Technical note: Dosimetric study of a new Co-60 source used in brachytherapy. *Medical Physics*. 2007;**34**:3485-3488. DOI: 10.1118/1.2759602
- [3] Guerrero R, Almansa JF, Torres J, Lallena AM. Dosimetric characterization of the ^{60}Co BEBIG Co0.A86 high dose rate brachytherapy source using PENELOPE. *Physica Medica*. 2014;**30**: 960-967. DOI: 10.1016/j.ejmp.2014.06.039
- [4] Anwarul IM, Akramuzzaman MM, Zakaria GA. Dosimetric comparison between the micro Selectron HDR ^{192}Ir v2 source and the BEBIG ^{60}Co source for HDR brachytherapy using the EGSnrc Monte Carlo transport code. *Journal of Medical Physics*. 2012;**37**(4): 219-225. DOI: 10.4103/2F0971-6203.103608
- [5] Badry H, Oufni L, Ouabi H, Hirayama HA. Monte Carlo investigation of the dose distribution for ^{60}Co high dose rate brachytherapy source in water and in different media. *Applied Radiation and Isotopes*. 2018;**136**: 104-110. DOI: 10.1016/j.apradiso.2018.02.016
- [6] Granero D, Perez-Calatayud J, Ballester F. Monte Carlo calculation of the TG-43 dosimetric parameters of a new BEBIG Ir-192 HDR source. *Radiotherapy and Oncology*. 2005;**76**: 79-85. DOI: 10.1016/j.radonc.2005.06.016
- [7] Granero D, Pérez-Calatayud J, Ballester F. Monte Carlo study of the dose rate distributions for the Ir2.A85-2 and Ir2.A85-1 Ir-192 afterloading sources. *Medical Physics*. 2008;**35**: 1280-1287. DOI: 10.1118/1.2868766
- [8] Belousov AV, Kalachev AA, Osipov AS. Monte Carlo Calculation of Dosimetry Parameters for a Brachytherapy Source. *Biophysics and Medical Physics*. 2014;**6**:95-100. DOI: 10.3103/S0027134914060034
- [9] Sechopoulos I, Rogers DWO, Bazalova-Carter M, Bolch WE, Heath EC, MF MN-G, et al. RECORDS: Improved Reporting of Monte Carlo Radiation transport Studies: Report of the AAPM Research Committee Task Group 268. *Medical Physics*. 2017;**45**(1): e1-e5. DOI: 10.1002/mp.12702
- [10] Alizadeh M, Ghorbani M, Haghparast A, Zare N, Moghaddas TA. A Monte Carlo study on dose distribution evaluation of Flexisource ^{192}Ir brachytherapy source. *Reports of Practical Oncology Radiotherapy*. 2015;**20**(3):204-209. DOI: 10.1016%2Fj.rpor.2015.01.006
- [11] Elboukhari S, Yamni K, Ouabi H, Bouassa T, Ait-Mlouk L. Technical note: Dosimetric study for the new BEBIG ^{60}Co HDR source used in brachytherapy in water and different media using Monte Carlo N-Particle eXtended code. *Applied Radiation and Isotopes*. 2020;**159**:109087. DOI: 10.1016/j.apradiso.2020.109087
- [12] Andrassy M, Niatsetsky Y, Pérez-Calatayud J. Controversies. ^{60}Co versus ^{192}Ir in HDR brachytherapy: Scientific

and technological comparison. *Revista Fis Medicina*. 2012;**13**(2):125-130

[13] Venselaar JL, van der Giessen PH, Dries WJ. Measurement and calculation of the dose at large distances from brachytherapy sources: Cs-137, Ir-192 and Co-60. *Medical Physics*. 1996;**23**: 537-543. DOI: 10.1118/1.597811

[14] Candela C, Perez-Calatayud J, Ballester F, Rivard MJ. Calculated organ doses using Monte Carlo simulations in a reference male phantom undergoing HDR brachytherapy applied to localized prostate carcinoma. *Medical Physics*. 2013;**40**:033901. DOI: 10.1118/1.4791647

[15] Strohmaier S, Zwierzchowski G. Comparison of ⁶⁰Co and ¹⁹²Ir sources in HDR brachytherapy. *Journal of Contemporary Brachytherapy*. 2011;**4**: 199-208. DOI: 10.5114/2Fjcb.2011.26471

[16] Ballester F, Granero D, Pérez-Calatayud J, Casal E, Puchades V. Monte Carlo dosimetric study of Best Industries and Alpha Omega Ir-192 brachytherapy seeds. *Medical Physics*. 2004;**31**(12): 3298-3305. DOI: 10.1118/1.1820013

[17] White MC. Further Notes on MCPLIB03/04 and New MCPLIB63/84. Compton Broadening Data For All Versions of MCNP5, LA-UR-12-00018. 2012

[18] Center NND. Nuclear data from NuDat, a webbased database maintained by the National Nuclear Data Center. Upton, NY, USA: Brookhaven National Laboratory; Available from: <http://www.nndc.bnl.gov/nudat2>

[19] Ballester F, Granero D, Pérez-Calatayud J, Casal E, Agramunt S, Cases R. Monte Carlo dosimetric study of the BEBIG Co-60 HDR source. *Physics in Medicine and Biology*. 2005;**50**(21):N309-N316. DOI: 10.1088/0031-9155/50/21/N03

[20] International Commission on Radiation Units and Measurements. Tissue Substitutes in Radiation Dosimetry and Measurement. ICRU Report no. 44. Bethesda, MD: International Commission on Radiation Units and Measurements; 1989

[21] Rivard MJ, Coursey BM, DeWerd LA, Hanson WF, Huq MS, Ibbott GS, et al. Update of AAPM Task Group No. 43 Report: A revised AAPM protocol for brachytherapy dose calculation. *Medical Physics*. 2004;**31**: 633-674. DOI: 10.1118/1.1646040

[22] Borg J, Rogers DW. Monte Carlo Calculations of Photon Spectra in Air from ¹⁹²Ir Sources. Ottawa, Canada, PIRS-629r: National Research Council; 1999

[23] Williamson JF. Monte Carlo evaluation of kerma at a point for photon transport problems. *Medical Physics*. 1987;**14**:567-576. DOI: 10.1118/1.596069

[24] Reyes E, Sosa M, Gil-Villegas A, Monzón E. Monte Carlo characterization of the Gamma Med HDRplus Ir-192 brachytherapy source. *Biomedical Physics & Engineering*. 2016;**2**:015017. DOI: 10.1088/2057-1976/2/1/015017

[25] Hubbell JH, Seltzer SM. Tables of X-Ray Mass Attenuation Coefficients and Mass Energy-Absorption Coefficients 1 keV to 20 MeV for Elements Z=1 to 92 and 48. Additional Substances of Dosimetric Interest. Gaithersburg, MD: NISTIR; 1995. p. 5632

[26] Granero D, Pérez-Calatayud J, Casal E, Ballester F, Venselaar J. A dosimetric study on the Ir-192 high dose rate Flexisource. *Medical Physics*. 2006;**33**:4578-4582. DOI: 10.1118/1.2388154